Nuclear Track Detectors. Searches for Exotic Particles

G. Giacomelli and V. Togo

Abstract We used Nuclear Track Detectors (NTD) CR39 and Makrofol for many purposes: (i) Exposures at the SPS and at lower energy accelerator heavy ion beams for calibration purposes and for fragmentation studies. (ii) Searches for GUT and Intermediate Mass Magnetic Monopoles (IMM), nuclearites, Q-balls and strangelets in the cosmic radiation. The MACRO experiment in the Gran Sasso underground lab, with $\sim$1,000 m^2 of CR39 detectors (plus scintillators and streamer tubes), established an upper limit for superheavy GUT poles at the level of 1.4×10^{-16} cm^{-2} s^{-1} sr^{-1} for $4 \times 10^{-5} < \beta < 1$. The SLIM experiment at the high altitude Chacaltaya lab (5,230 m a.s.l.), using 427 m^2 of CR39 detectors exposed for 4.22 years, gave an upper limit for IMMs of $\sim 1.3 \times 10^{-15}$ cm^{-2} s^{-1} sr^{-1}. The experiments yielded interesting upper limits also on the fluxes of the other mentioned exotic particles. (iii) Environmental studies, radiation monitoring, neutron dosimetry.

Keywords: Nuclear track detectors, Magnetic Monopoles, nuclearites, Q-balls

1 Introduction

Nuclear Track Detectors are used in many branches of science and technology [1]. The isotropic poly-allyl-diglycol carbonate polymer, commercially known as CR39, is the most sensitive NTD; also Makrofol and Lexan polycarbonates are largely employed.

G. Giacomelli
University of Bologna and INFN Bologna, Italy,
e-mail: giacomelli@bo.infn.it

V. Togo
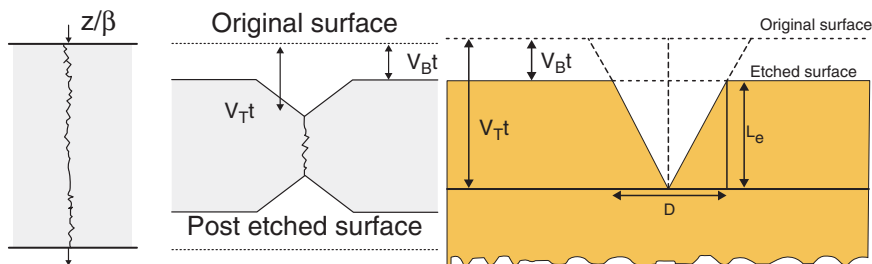INFN, Sezione di Bologna, Italy,
e-mail: togo@bo.infn.it

Fig. 1 Sketch of: (a) The latent track formation by a charged particle passing in a NTD. (b) Situation after etching. (c) Parameters of an etched track for a normally incident fast ion in a NTD

A nuclear track detector records the passage of highly ionizing particles via their Restricted Energy Loss (REL). The latent damage trail formed in NTDs may be enlarged by a suitable chemical etching and made visible under an optical microscope. The latent track develops into a conical-shaped etch-pit (Fig. 1) when the etching velocity along the particle trajectory (v_T) is larger than the bulk etching velocity of the material (v_B) [2]. The sensitivity of NTDs crossed by particles with constant energy loss is characterized by the ratio $p = v_T/v_B$ (reduced etch rate) which is determined by measuring the bulk etch rate v_B and either the etch-pit diameter or height. Two methods were used to determine v_B. The first is the common one based on the mean thickness difference before and after etching. The second method is based on both cone height and base diameter measurements of the etched tracks.

The measured track diameter D and track length L_e are expressed in terms of the velocities v_T and v_B

$$D = 2v_B t \sqrt{\frac{(v_T - v_B)}{(v_T + v_B)}} \tag{1}$$

$$L_e = (v_T - v_B)t \tag{2}$$

from which one obtains

$$p = \frac{v_T}{v_B} = 1 + \frac{L_e}{v_B t} = \frac{1 + (\frac{D}{2v_B t})^2}{1 - (\frac{D}{2v_B t})^2} \tag{3}$$

Experiments in different fields require an accurate detector calibration [3, 4]. More than 4,000 m^2 of CR39 detectors were used in the MACRO and SLIM experiments which searched for new massive particles in the cosmic radiation (Magnetic Monopoles, nuclearites, Q-balls) [5–13].

In this note will be summarized the technical work on NTDs and results on fragmentation studies, on the search for MMs, nuclearites and Q-balls in the cosmic radiation, underground or at high altitudes, and environmental monitoring.

2 Experimental. Calibrations

Stacks composed of CR39 and Makrofol foils of size 11.5×11.5 cm^2 with several targets were exposed to 158 A GeV In^{49+} ions in 2003 at the CERN-SPS, at normal incidence and a total ion density of $\sim$2,000 /cm^2. The detector foils downstream of the target recorded the beam ions as well as their nuclear fragments [14–16] see Fig. 2. The CR39 polymer sheets were manufactured by Intercast Europe Co., Parma, Italy, where a scientific production line was set up in order to achieve a lower detection threshold, a higher sensitivity in a larger range of energy losses, a high quality of the post-etched surfaces after prolonged etching [17, 18]. The Makrofol detectors were manufactured by Bayer A.G., Germany.

After exposures, CR39 and Makrofol foils located after the target were etched in 6N NaOH + 1% ethyl alcohol at 70°C for 40 h and 6N KOH + 20% ethyl alcohol at 50°C for 8 h that are the optimum etching condition for CR39 and Makrofol, respectively. The addition of ethyl alcohol in the etchant improves the etched surface quality, reduces the number of surface defects and background tracks, increases the bulk etching velocity, speeds up the reaction, but raises the detection threshold [11, 19]. The etching was performed in a stainless steel tank equipped with internal thermo-resistances and a motorized stirring head. A continuous stirring was applied; the temperature was stable to within ±0.1°C.

Figure 3a shows the etch-pit base area distribution for indium ions and their fragments in CR39 measured with the Elbek image analyzer system [20]; averages were computed from measurements made on the "front sides" of two detector sheets. The fragment peaks are well separated, from $Z/\beta \sim 7$ to 45; the charge resolution for the average of two measurements is $\sigma_Z \sim 0.13$e at $Z/\beta \sim 15$. The resolution close to the indium peak (Z = 49) can be improved by measuring the heights of the etch-pit cones [21].

They were measured with a Leica microscope coupled to a CCD camera and a video monitor; the L_e distribution is shown in the insert in Fig. 3a [19]. For each nuclear fragment we computed the REL and the reduced etch rate p using Eq. 3; p vs REL is plotted in Fig. 3b; the CR39 detection threshold is at REL$\sim$50 MeV cm^2 g^{-1} (corresponding to a relativistic fragment with $Z/\beta \sim 7$).
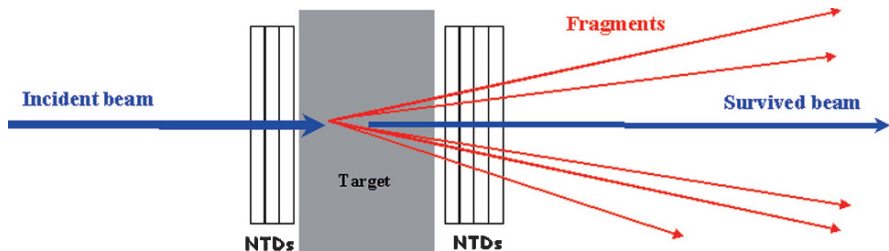

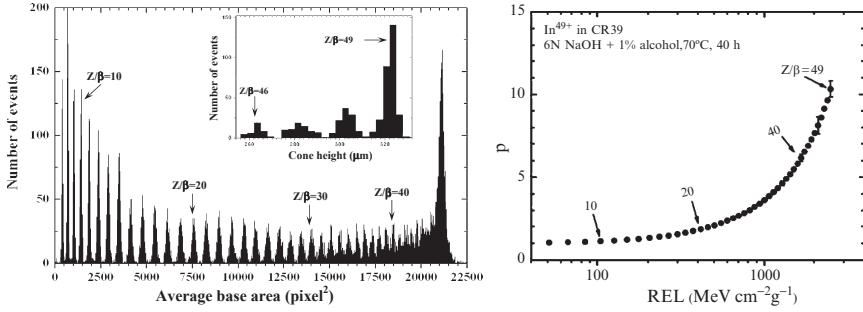**Fig. 2** Exposure set-up for the calibration of CR39 and Makrofol NTDs

Fig. 3 (a) Base area distributions of etched cones in CR39 from 158 A GeV In^{49+} ions and their fragments. In the insert are shown the cone height distribution for $46 \leq Z/\beta \leq 49$. (b) p vs REL for CR39; statistical standard deviations are shown at $Z/\beta = 40, 45, 49$; for $Z/\beta < 37$ the errors are smaller than the size of the points
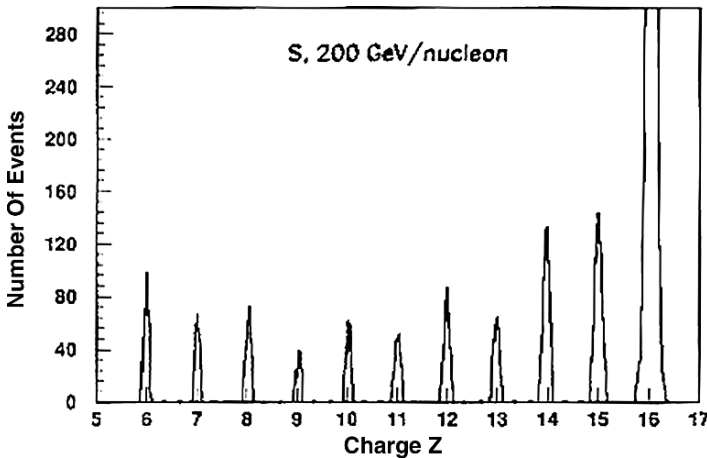

Fig. 4 Search for nuclear fragments with fractional charges in CR39 detectors (12 measurements were made on the same track)

Measurements of *Makrofol detectors* exposed to Pb ions and their fragments yield fragmentation peaks well separated from $Z/\beta \sim 51$ to ~ 77. The threshold is at $Z/\beta \sim 50$; the charge resolution for 2 face measurement is $\sigma_Z \sim 0.18e$ at $Z/\beta \sim 55$.

Figure 4 shows the results of repeated precision measurements on the same track (12 times) in CR39 detectors exposed to 200 GeV/nucleon S ions and their fragments. The charge resolution is adequate to allow a search for fragments with fractional charges. The limits on fractional charge fragments are at the level of 10^{-4} [22].

3 Fragmentation cross sections

The availability of ion beams at CERN, BNL and Chiba (HIMAC) made possible to investigate the projectile fragmentation on different targets and for rather different projectile energies. The total charge changing cross sections were determined from the survival fraction of ions using the following relation

$$\sigma_{tot} = \frac{A_T \ln(N_{in}/N_{out})}{\rho \ t \ N_{Av}} \tag{4}$$

where A_T is the nuclear mass of the target; N_{in} and N_{out} are the numbers of incident ions before and after the target, respectively; ρ (g/cm^3) is the target density; t (cm) is the target thickness and N_{Av} is Avogadro number.

At low energies the total fragmentation cross sections are essentially energy independent and are in agreement with semi-empirical formula [23]. At high energies the fragmentation cross section depends on the target mass as $\sim A_T^{1/3}$. The partial fragmentation cross sections increase with decreasing ΔZ and the cross sections leading to even Z fragments are slightly larger than those leading to odd Z [14, 15].

4 Searches for magnetic monopoles

GUT theories of the electroweak and strong interations predict the existence of superheavy MMs produced in the Early Universe when the GUT gauge group breaks into separate groups, one of which is U(1):

$$SU(5) \quad \underset{10^{-35} \text{ s}}{\overset{10^{15} \text{ GeV}}{\longrightarrow}} \quad SU(3)_C \times [SU(2)_L \times U(1)_Y] \quad \underset{10^{-9} \text{ s}}{\overset{10^2 \text{ GeV}}{\longrightarrow}} \quad SU(3)_C \times U(1)_{EM} \tag{5}$$

MMs should be generated as topological point defects in the GUT phase transition $SU(5) \longrightarrow U(1)_Y$, about one pole for each causal domain. In standard cosmology this leads to too many poles (*the monopole problem*). A rapid expansion of the early Universe (*inflation*) would defer the GUT phase transition; in the simplest inflation version the number of generated MMs is small. However if there was a reheating phase one may have MMs produced in high energy collisions, like $e^+e^- \to M\bar{M}$.

Figure 5 shows a sketch of the energy loss of a MM in liquid H.

The structure of a GUT MM: a very small core, an electroweak region, a confinement region, a fermion–antifermion condensate (which may contain 4-fermion baryon–number–violating terms); for $r \geq$ few fm a GUT pole behaves as a point particle generating a field $B = g/r^2$, Fig. 6 [9].

A flux of cosmic GUT MMs may reach the Earth with a velocity spectrum in the range $4 \times 10^{-5} < \beta < 0.1$, with possible peaks corresponding to the escape velocities from the Earth, the Sun and the Galaxy. Searches in the Cosmic Rays (CR) performed with superconducting induction devices yielded a 90% CL limit of 2×10^{-14} cm^{-2} s^{-1} sr^{-1} independent of β [24].
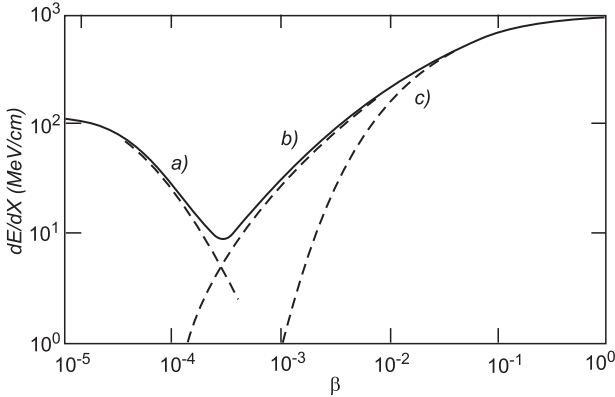
Fig. 5 The energy losses of $g = g_D$ MMs in liquid hydrogen due to (a) elastic collisions; (b) excitation and Drell effect; (c) ionization
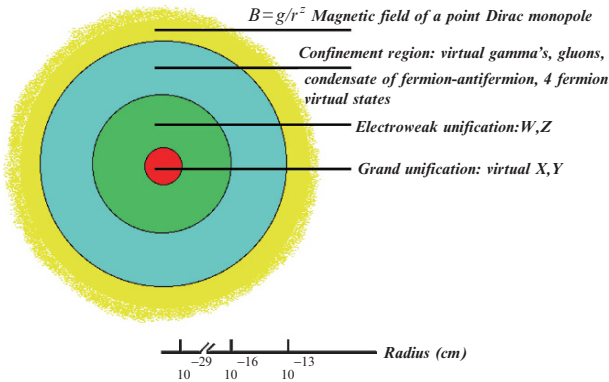

Fig. 6 Extended picture of a GUT Magnetic Monopole

Direct searches were performed above ground and underground [9, 25, 26]. MACRO made a search with liquid scintillators, limited streamer tubes and NTDs; the 90% CL flux limits obtained with the NTDs are shown in Fig. 7a. Figure 7b shows the limits for $g = g_D$ obtained with all the subdetectors; they are at the level of 1.4×10^{-16} cm^{-2} s^{-1} sr^{-1} for $\beta > 4 \times 10^{-5}$ [5, 27]. The figure shows also the limits from the Ohya, Baksan, Baikal, and AMANDA experiments [28].

Indirect GUT MM searches used ancient mica which is a NTD with a very high threshold. It is assumed that a pole passing through the Earth captures an Al nucleus and drags it through subterranean mica causing lattice defects, which survive as long as the mica is not reheated. Only small sheets were analyzed (13.5 and 18 cm^2), but they recorded tracks for $4 \div 9 \times 10^8$ year. The flux limits are at the level of $\sim 10^{-17}$ cm^{-2} s^{-1}sr^{-1} for $10^{-4} < \beta < 10^{-3}$ [29]. But these indirect experiments might not be really so sensitive.
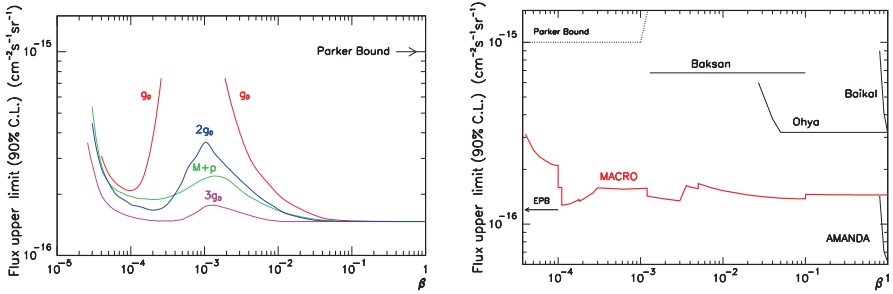
Fig. 7 (a) Upper limits (90%) for an isotropic flux of MMs obtained with the CR39 subdetector of MACRO for poles with magnetic charge g = g$_D$, 2g$_D$, 3g$_D$ and for M+p composites. (b) Global limit obtained by MACRO for GUT poles with g = g$_D$, using all its subdetectors

Intermediate Mass Magnetic Monopoles may appear as topological point defects at a later time in the Early Universe, *i.e.* if the GUT group yields the U(1) group of the Standard Model in the following two steps:

$$SO(10) \quad \overset{10^{15} \text{ GeV}}{\underset{10^{-35} \text{ s}}{\longrightarrow}} \quad SU(4) \times SU(2) \times SU(2) \quad \overset{10^{9} \text{ GeV}}{\underset{10^{-23} \text{ s}}{\longrightarrow}} \quad SU(3) \times SU(2) \times U(1) \qquad (6)$$

This would lead to MMs with masses of $\sim 10^{10}$ GeV; they would survive inflation, be stable, "doubly charged" $(g = 2g_D)$ and do not catalyze nucleon decay [30]. The structure of an IMM is similar to that of a GUT MM, but the core is larger.

Relativistic IMMs with masses, $10^7 < m_M < 10^{13}$ GeV, may be present in the cosmic radiation, and may be accelerated to high γ factors in one domain of the galactic magnetic field. Detectors at the Earth surface may detect downgoing IMMs if $m_M > 10^5$ GeV [9]; lower mass MMs may be detected at high mountain altitudes, in balloons and in satellites.

SLIM at 5230 m a.s.l. [6] was based on 427 m^2 of CR39 and Makrofol detectors exposed for 4.27 years to the CR. The detectors were organized in modules of 24 × 24 cm^2, each consisting of three layers of CR39 interleaved with three layers of Makrofol and 1 mm Al absorber. Each module was packed in an aluminized polyethylene envelope at 1 atm of dry air to prevent the CR39 loss in sensitivity at a reduced oxygen content in the air (0.5 atm). The 90% CL flux upper limits for downgoing IMMs with $g = g_D$, 2g$_D$, 3g$_D$ and M+p are plotted in Fig. 8 vs β (2g$_D$ is the theoretically preferred value).

5 Searches for nuclearites, strangelets, Q-balls

Strange Quark Matter (SQM) consists of aggregates of *u*, *d* and *s* quarks in almost equal proportions (the number of *s* quarks is lower than the number of *u* or *d* quarks and SQM should have a relatively small positive integer charge).
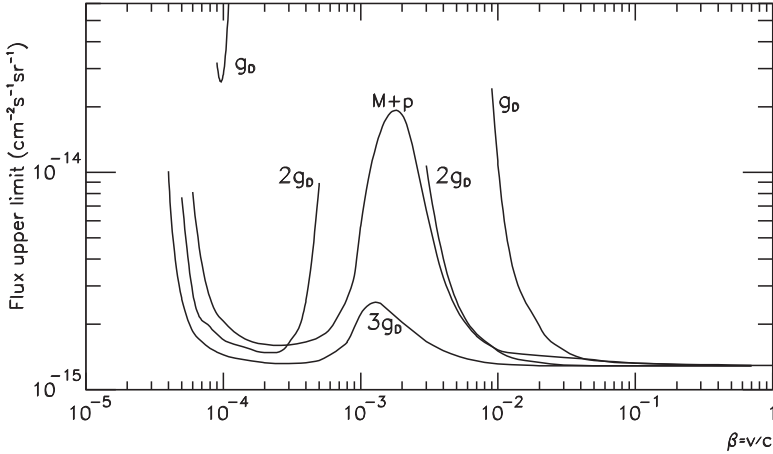
Fig. 8 90% CL upper limits from the SLIM experiment on IMMs in the cosmic radiation

$R_N = 10^2$ fm $R_N = 10^3$ fm $R_N = 10^4$ fm $R_N = 10^5$ fm $R_N = 10^6$ fm
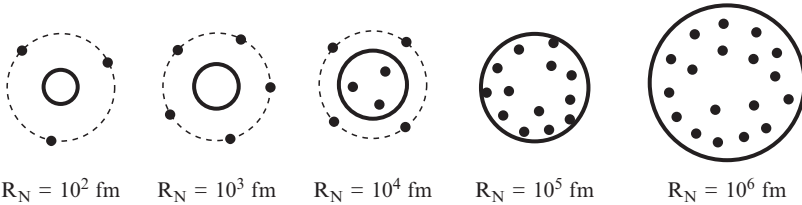
Fig. 9 Sketch of nuclearite structure: the quark bag radius R_N and the core plus electron system (indicated by dashed lines); the electrons are indicated by black points

The overall neutrality of SQM is ensured by an electron cloud which surrounds it, forming a sort of atom, see Fig. 9 [9, 31–33]. SQM has a constant density $\rho_N = M_N/V_N \simeq 3.5 \times 10^{14}$ g cm^{-3}, slightly larger than that of atomic nuclei, and it should be stable for all baryon numbers between ordinary heavy nuclei and neutron stars. SQM with baryon number $A < 10^6 - 10^7$ are called "*strangelets*"; the word "*nuclearite*" was introduced to indicate larger lumps of SQM, which may be present in the Cosmic Radiation [12,31,32]. SQM may have been produced shortly after the Big Bang and may have survived as remnants. SQM may contribute to the cold Dark Matter (DM) in the Universe.

The main energy loss for low velocity nuclearites is due to elastic or quasi-elastic collisions with ambient atoms. The loss is large; therefore nuclearites may be easily detected in scintillators and CR39 NTDs. Nuclearites should have typical galactic velocities, $\beta \sim 10^{-3}$, and for masses >0.1 g could traverse the Earth.

Most nuclearite searches were made as byproducts of CR MM searches; the flux limits are similar to those for MMs. Direct flux limits for nuclearites come from large area experiments with CR39 NTDs; Mt. Norikura at 2,770 m a.s.l. [28]; at the depth of $\sim 10^4$ g cm^{-2} in the Ohya mine [28]; MACRO, at a depth of 3,700 hg cm^{-2}, used also liquid scintillators [33]. Experimental limits for heavy nuclearites are at
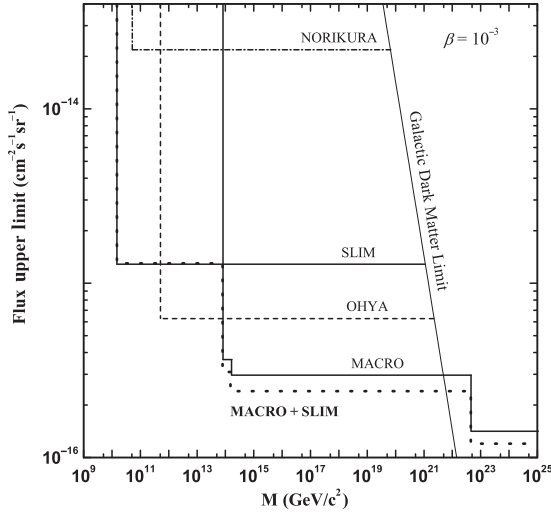
Fig. 10 Flux limits at 90% CL for downgoing nuclearites vs mass

the level of those presented in Fig. 7b for GUT MMs: $\sim 1.4 \times 10^{-16}$ cm^{-2} s^{-1} sr^{-1}. For Intermediate Mass Nuclearites the limits are at the level indicated in Fig. 7a. For small nuclearites, $A < 8,000$, the predicted flux in the cosmic radiation is expected to increase with decreasing mass. The present status of the search for galactic nuclearites is summarized in Fig. 10 [13,32]. Indirect searches may yield lower limits, but they are affected by systematic uncertainties. Some exotic cosmic ray events were interpreted as due to incident nuclearites, f. e. the "Centauro" events and the anomalous massive particles, but the interpretation is not unique [34].

Q-balls should be aggregates of squarks $\tilde{q}$, sleptons $\tilde{l}$ and Higgs fields [35]. The scalar condensate inside a Q-ball core has a global baryon number Q (and may be also a lepton number). Protons, neutrons and electrons may be absorbed in the condensate. There may be neutral and charged Q-balls: Supersymmetric Electrically Neutral Solitons (SENS) (more massive and may catalyse proton decay); SENS may obtain a positive electric charge when absorbing a proton in their interaction with matter yielding SECS (Supersymmetric Electrically Charged Solitons), which have a core electric charge and lower masses; the Coulomb barrier may prevent the capture of nuclei. SECS have only integer charges because they are color singlets. Figure 11 [32] shows sketches of SECS and SENS. A SENS which enters the Earth atmosphere could absorb a nitrogen nucleus and become a SECS with charge $Z_Q = 7$. Q-balls could be cold DM candidates. SECS with $\beta \sim 10^{-3}$ and $M_Q < 10^{13}$ GeV may reach an underground detector from above. SENS may be detected by their large emission of pions; SECS may be detected by scintillators, NTDs and ionization detectors. Figure 12 shows the present status of the searches for galactic charged Q-balls with a net charge $Z_Q = 1$.
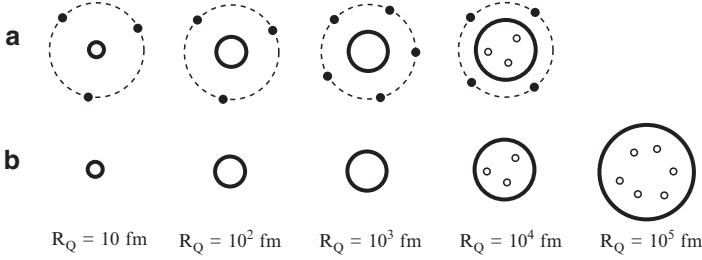
Fig. 11 Sketch of supersymmetric Q-ball structure: (a) for SECS and (b) for SENS. The black points are electrons, the empty dots are s-electrons
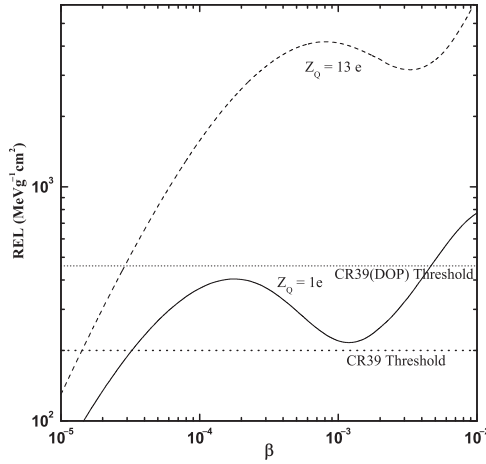

Fig. 12 REL vs β for downgoing charged Q-balls (SECS)

6 Conclusions. Outlook

The NTDs CR39 and Makrofol were calibrated with different ions of different energies. For each type of detector a unique curve of p vs REL describes their response.

The total fragmentation cross sections for low energy ions on different targets do not show any observable energy dependence and are in agreement with similar data in the literature.

Direct and indirect accelerator searches for classical Dirac MMs placed limits for $m_M \leq 800$ GeV. Future improvements may come from LHC experiments [36]. Searches performed for GUT poles in the penetrating cosmic radiation yielded 90% CL flux limits at the level of $\sim 1.4 \times 10^{-16}$ cm^{-2} s^{-1} sr^{-1} for $\beta \geq 4 \times 10^{-5}$. Present limits on IMMs with high β, in the downgoing cosmic radiation are at the level of 1.3×10^{-15} cm^{-2} s^{-1} sr^{-1}. As a byproduct of GUT MM searches some experiments obtained stringent limits on nuclearites, strangelets and Q-balls.

In the past, a number of monopole and of other exotic candidates were thought to have been observed and some results were published [34, 37]. But they were

not confirmed and most of them are now neglected. In 2006 the SLIM experiment faced a problem of this type when analysing the top faces of the top CR39 layers. A sequence of etch-pits was found along a ∼20 cm line; each one of them looked complex and very different from usual ion tracks. Since the "candidate event" was rather peculiar, a thorough study was made in all the sheets of the module, and in all NTD sheets in the modules within a ∼1 m distance. Short soft etching periods were used so as to follow the evolution of the etch-pits. It was concluded that they originated in a rare manufacturing defect involving 1 m^2 of CR39 [38].

We measured the radon concentration in the houses of the city of Bologna, in the Gran Sasso Underground Laboratory and in some thermal sites. In the first two cases the radon level was globally low, and changed with the floor and ventilation [39]. At the 2008 24th Int. Conf. on Nuclear Tracks in Solids, in Bologna, new results were presented in Radiation Environment Monitoring (mainly radon), Neutron Dosimetry and Medical Applications (see proceedings in Radiation Measurements).

References

1. S.A. Durrani et al., Solid State Nuclear Track Detection, Pergamon, Oxford (1987).
2. D. Nikezic et al., Material Science Eng. R **46** (2004) 51.
3. Y. Uchihori et al., J. Radiat. Res. **43** (Suppl. S81-5) (2002).
4. S. Kodaira et al., Jpn. J. Appl. Phys. **43** (2004) 6358.
5. M. Ambrosio et al., Eur. Phys. J. C **25** (2002) 511; Nucl. Instrum. Meth. A **486** (2002) 663.
6. S. Balestra et al., Eur. Phys. J. C **55** (2008) 57; hep-ex/0506075; hep-ex/0602036. V. Togo and I. Traoré, arXiv:0811.2885 [physics.ins-det].
7. S. Cecchini et al., astro-ph/0510717 (2005).
8. S. Cecchini et al., Radiat. Meas. **40** (2005) 405.
9. J. Derkaoui et al., Astropart. Phys. **10** (1999) 339. D. Bakari et al., hep-ex/0004019.
10. G. Giacomelli et al., hep-ex/0702050 (2007).
11. S. Manzoor et al., Nucl. Phys. B (Proc. Suppl.) **172** (2007) 296.
12. E. Medinaceli, arXiv:0811.1111 [hep-ex].
13. Z. Sahnoun, 24th Int. Conf. Nucl. Tracks in Solids, (2008) Bologna, Radiat. Meas.
14. S. Cecchini et al., Nucl. Phys. A **807** (2008) 206.
15. M. Giorgini, arXiv:0812.0236 [nucl-ex]; arXiv:0812.0685 [physics.ins-det].
16. V. Togo et al., Nucl. Instrum. Meth. A **580** (2007) 58.
17. L. Patrizii et al., Nucl. Tracks Radiat. Meas. **19** (1991) 641.
18. E. Vilela et al., Radiat. Meas. **31** (1999) 437.
19. S. Balestra et al., Nucl. Instrum. Meth. B **254** (2007) 254.
20. A. Noll et al., Nucl. Tracks Radiat. Meas. **15** (1988) 265.
21. G. Giacomelli et al., Nucl. Instrum. Meth. A **411** (1998) 41.
22. S. Cecchini et al., Astropart. Phys. **1** (1993) 369.
23. H.L. Bradt et al., Phys. Rev. **77** (1950) 54. S. Cecchini et al., Nucl. Phys. A **707** (2002) 513.
24. G. Giacomelli et al., hep-ex/011209; hep-ex/0302011; hep-ex/0211035; hep-ex/0506014.
25. J. Ruzicka and V.P. Zrelov JINR-1-2-80-850 (1980).
26. G. Giacomelli et al., hep-ex/0005041.

27. M. Ambrosio et al., Phys. Lett. B **406** (1997) 249; Astropart. Phys. **18** (2002) 27.
28. S. Orito et al., Phys. Rev. Lett. **66** (1991) 1951. Yu.F. Novoseltsev et al., Nucl. Phys. B **151** (2006) 337. V. Aynutdinov et al.,astro-ph/0507713. A. Pohl et al., astro-ph/0701333.
29. P.B. Price, Phys. Rev. D **38** (1988) 3813. D. Ghosh et al., Europhys. Lett. **12** (1990) 25.
30. T.W. Kephart and Q. Shafi, Phys. Lett. B **520** (2001) 313.
31. E. Witten, Phys. Rev. D **30** (1984) 272. A. De Rujula and S. Glashow, Nature **31** (1984) 272.
32. S. Cecchini et al., arXiv:0805.1797 [hep-ex].
33. M. Ambrosio et al., Eur. Phys. J. C **13** (2000) 453. S. Ahlen et al., Phys. Rev. Lett. **69** (1992) 1860.
34. M. Rybczynski et al., hep-ph/0410064. D. P. Anderson et al., astro-ph/0205089
35. S. Coleman, Nucl. Phys. B **262** (1985) 293. A. Kusenko et al., Phys. Lett. B **418** (1998) 46.
36. G. Abbiendi et al., Phys. Lett. B **663** (2008) 37.
37. P.B. Price et al., Phys. Rev. Lett **35** (1975) 487; Phys. Rev. D **18** (1978) 1382.
38. S. Balestra et al., arXiv:0802.2056 [hep-ex].
39. G. Giacomelli et al., Il Nuovo Saggiatore **4** (1990) 5; Acqua Aria **4** (1990) 371. C. Arpesella et al., Health Phys. **72** (1997) 629.